HHS Public Access

Author manuscript

J Cell Biochem. Author manuscript; available in PMC 2021 June 18.

Published in final edited form as:

J Cell Biochem. 2017 March ; 118(3): 585–593. doi:10.1002/jcb.25739.

REAL-TIME H_2O_2 MEASUREMENTS IN BONE MARROW MESENCHYMAL STEM CELLS (MSCs) SHOW INCREASED ANTIOXIDANT CAPACITY IN CELLS FROM OSTEOPOROTIC WOMEN

Flavia Román[1], **Carla Urra**[1], **Omar Porras**[1], **Ana María Pino**[1], **Clifford J. Rosen**[2], **J. Pablo Rodríguez**[1,*]

[1]Laboratorio de Biología Celular. Instituto de Nutrición y Tecnología de los Alimentos. Universidad de Chile.

[2]Maine Medical Center Research Institute, Scarborough, Maine, USA

Abstract

Oxidative stress (OS) derived from an increase in intracellular reactive oxygen species (ROS) is a major determinant of aging and lifespan. It has also been associated with several age-related disorders, like postmenopausal osteoporosis. Mesenchymal stem cells (MSCs) are the common precursors for osteoblasts and adipocytes; appropriate commitment and differentiation of MSCs into a specific phenotype is modulated, among other factors, by ROS balance. MSCs have shown more resistance to ROS than differentiated cells, and their redox status depends on complex and abundant anti-oxidant mechanisms. The purpose of this work was to analyze in real time, H_2O_2 signaling in individual h-MSCs, and to compare the kinetic parameters of H_2O_2 management by cells derived from both control (c-) and osteoporotic (o-) women. For these purposes, cells were infected with a genetically encoded fluorescent biosensor named HyPer, which is specific for detecting H_2O_2 inside living cells. Subsequently, cells were sequentially challenged with 50 μM and 500 μM H_2O_2 pulses, and the cellular response was recorded in real time. The results demonstrated adequate expression of the biosensor allowing registering fluorescence from HyPer at a single cell level. Comparison of the response of c- and o-MSCs to the oxidant challenges demonstrated improved antioxidant activity in o-MSCs. This was further corroborated by measuring the relative expression of mRNAs for catalase, superoxide dismutase-1, thioredoxine and peroxiredoxine, as well as by cell-surviving capacity under short-term H_2O_2 treatment. We conclude that functional differences exist between healthy and osteoporotic human MSCs. The mechanism for these differences requires further study.

Keywords

Mesenchymal stem cells; Osteoporosis; Antioxidant capacity

[*]Correspondence to: J. Pablo Rodríguez PhD, Laboratorio de Biología Celular. Instituto de Nutrición y Tecnología de los Alimentos. Universidad de Chile, Av. El Líbano 5524, Macul, Santiago, Chile. jprodrig@inta.uchile.cl.

Introduction

Osteoporosis is a metabolic bone disease characterized by both decreased bone quality and mineral density. In postmenopausal osteoporosis, increased bone fragility and susceptibility to fractures result from increased osteoclastogenesis, inadequate osteoblastogenesis and altered bone microarchitecture. The pathogenesis of the disease is hitherto under debate; the activities of several cell types including osteocytes, osteoclasts and osteoblasts as well as the differentiation potential of mesenchymal stem cells (MSCs) play a role in the course of the disease [Pino et al, 2012].

MSCs are the common precursors for osteoblasts and adipocytes; therefore, preserving bone tissue requires adequate osteoblast formation at the expense of adipogenesis. Commitment and differentiation of MSCs into a specific phenotype *in vivo* is controlled by both intrinsic (genetic) and environmental (local and/or systemic) conditions that define cell fate. Factors like age [Zhou et al, 2008], culture condition [Kultere et al, 2007], microenvironment [Kuhn and Tuan, 2010], mechanical strain [McBride et al, 2008] and other pathologies [Seebach et al, 2007; Hofer et al, 2010] appear to affect the intrinsic activity of MSCs.

Normal cellular metabolism generates low levels of some oxygen-derived molecules called reactive oxygen species (ROS), which are scavenged by antioxidant mechanisms of the cells [Manolagas, 2010; Filaire and Toumib, 2012]. Balanced levels of ROS modulate key metabolic functions by playing a role in intracellular signaling [Bai et al, 2005; Iyer et al, 2013; Manolagas and Almeida, 2007]. In several conditions such as ageing, tissue inflammation, tumor and degeneration, the redox homeostasis shifts towards an oxidative status as a result of increase in ROS production and/or impairment in antioxidant mechanism, resulting in oxidative stress [Valko et al, 2007; Serafini, 2006; McCord, 2000; Dalle-Donne et al, 2006]. Importantly, ROS generation is essential for adipogenic but not osteogenic differentiation; indeed, high levels of ROS can suppress oxidative phosphorylation [Wang et al, 2015; Atashi et al, 2015].

Oxidative stress (OS) derived from an increase in intracellular ROS is the major determinant of aging and lifespan [Harman, 1956; Giorgio et al, 2007; Russell and Kahn, 2007; Lu and Finkel, 2008], as well as the source in several degenerative age-related disorders [Balaban et al, 2005]. Cells have developed diverse mechanisms to prevent, repair or defend from the effects of excessive ROS production. Enzymatic antioxidant defenses include superoxide dismutases (SOD) [Afonso et al, 2007], catalase, and glutathion peroxidases. Non-enzymatic antioxidants include thioredoxins, peroxiredoxins and a variety of free radicals quenchers such as ascorbic acid, - tocopherol, carotenoids, flavonoids, thiols which include glutathione, ubiquinone Q 10, uric acid, bilirubin, ferritin and micronutrients which act as enzymatic cofactors [Manolagas, 2010; Atashi et al, 2015].

OS is a distinctive environmental bone marrow condition that has harmful effects on bone [Maggio et al, 2003; Feng and Tang, 2014]; epidemiological evidence in humans and current mechanistic studies in rodents sustain that aging and the associated increase in ROS play a role in the pathogenesis of osteoporosis [Manolagas, 2010; Maggio et al, 2003; Basu et al, 2001; Oh et al, 2007]. Experimental studies in bone cells showed that ROS, particularly

H_2O_2, or depletion of GSH suppress osteoblastic differentiation of bone marrow cells [Bai et al, 2005], whereas osteoblast apoptosis induced by OS *in vitro* is attenuated by glutaredoxin 5 [Linares et al, 2009]. Oxidative stress interacts with other regulatory signals in bone cells, thus it induces FoxO transcription factors to activate essential genes for ROS scavenging. The activation of FoxO transcription factors inactivates Wnt signaling as well, disrupting bone formation [Iyer et al, 2013; Manolagas and Almeida, 2007; Ambrogini et al, 2010; Rached et al, 2010]. In addition, the formation of oxidized lipids through ROS activates PPARγ signaling in MSCs, enhancing adipogenesis, thereby diminishing bone formation [Manolagas, 2010; Almeida et al, 2009].

Stem cells have shown more resistance to ROS than differentiated cells, and preserving their redox status depends on complex and plentiful anti-oxidant tools [Atashi et al, 2015; Mouzannar et al, 2011; Valle-Prieto and Conget, 2010], thus implicating the significance of accurate management of OS for all stem cells, especially when considering that *in vivo* stem cells have a long lifespan and are exposed to OS for long periods of time.

Defining the response of stem cells to ROS is critical to understanding the distinctive sensitivity of these cells to these agents and whether a disease condition affects such features. Current evidence has evaluated the response to ROS in stem cells populations, although there are mechanistic questions in respect to detect ROS directly in living cell, thus requiring sensitive procedures.

Recently, a genetically encoded fluorescent biosensor named HyPer has been developed, which is specific for detecting H_2O_2 inside living cells. HyPer is derived from the OxyR transcription factor found in E. *coli* with YFP inserted between two reactive thiol groups to provide a fluorescent readout of critical cysteine residues oxidation state on the OxyR [Belousov et al, 2006]. Once the biosensor is expressed by the target cell, its fluorescent spectra changes upon reaction with hydrogen peroxide only- it is unresponsive to other oxidants- allowing ratiometric signal recording. Unlike the read- outs in other intracellular ROS sensing strategies [Kalyanaraman et al, 2012], HyPer signal is reversible due to the activity of intracellular reductases, and this feature allows peroxide levels to be monitored in real-time.

This work focused on studying the antioxidant status of bone marrow MSCs derived from both control and osteoporotic women, by registering *in vivo* H_2O_2 signaling in individual cells expressing the HyPer sensor. For this purpose, both types of cells were infected with the HyPer biosensor prior to a H_2O_2 challenge, and the subsequent cellular response was recorded in real time. The results demonstrated adequate expression of the biosensor allowing registering fluorescence from HyPer at single cells level, showing remarkable dynamic differences between c- and o-MSCs in their response to consecutive oxidant challenges, suggesting improved antioxidant activity in o-MSCs. This conclusion was further corroborated by measuring the relative expression of mRNAs for main cellular antioxidant mechanisms, as well as by cells surviving capacity under short-term H_2O_2 treatment.

Materials and Methods

Subjects

Postmenopausal women aged 60 to 75 years old who required bone surgery due to hip fracture or arthroplasty, at the Trauma Section of Hospital Sótero del Río, Santiago, Chile, were asked to volunteer as bone marrow donors. Bone marrow samples were obtained by iliac crest aspiration during surgical procedures [Astudillo et al, 2008]. Written informed consent was obtained from all subjects and ethical approval was obtained from the respective Instituto de Nutrición y Tecnología de los Alimentos (INTA) and Hospital Sótero del Río ethics committees. For each subject, bone mineral density (BMD) was measured within 4 weeks after surgery by dual-energy X-ray absorptiometry (DXA) (LUNAR, Prodigy, General Electric Medical Systems, Madison, WI, USA). Donors were classified as control or osteoporotic according to their BMD value (Table 1); control donors had BMD higher than −1.0 standard deviations (SD) of the mean BMD for young adults and osteoporotic donors had BMD lower than −2.5 SD [Raiz, 1997]. Control (t-score = −0.63 ± 0.81) and osteoporotic (t-score = −3.68 ± 0.7) donors considered themselves healthy, except for the fractures, and were not under bisphosphonates, glucocorticoid or estrogen therapy.

Cell preparation and culture methods

MSCs were classified as control (c-MSCs) or osteoporotic (o-MSCs) according to whether they derived from control or osteoporotic donors. MSCs were isolated from bone marrow as previously described [Jaiswal et al, 1997]. Briefly, 10 ml of bone marrow aspirate were added to 20 ml of Dulbecco's Modified Eagle medium high glucose containing 10% fetal bovine serum (basal medium) and was centrifuged to pellet the cells, discarding the fat layer. Cells were re-suspended in basal medium and fractionated on a 70% Percoll density gradient. The MSCs-enriched low-density fraction was collected, rinsed with basal medium and plated at a density of 1–2 × 10^7 nucleated cells/100 mm dishes. Cells were cultured at 37°C in a humidified atmosphere of 5% CO_2. After 4 days in culture, non-adherent cells were removed and fresh culture medium was added. Basal medium was replaced by fresh medium twice weekly. When culture dishes reached near confluence, cells were detached by mild treatment with trypsin (0.25%, 5 min, 37°C) and plated at 1/3 the original density to allow for continued passage. The experiments described here were performed after the fourth cell passage.

Virus production and cell infection

Adenoviral vector was generated using the AdEasy system. Briefly, cDNA of cyto-HyPer (Evrogen, Moscow, Russia) was sub-cloned into the commercial adenoviral vector pAdEasy-RFP with conventional molecular biology techniques, and homologous recombination was done by BJ5183 cells transformation. Recombinant adenoviral plasmid was digested with PacI and transfected in AdHek cells with lipofectamine using manufacturer guidelines (Invitrogen, Carlsbad, CA, USA). Following observation of cytopathic effects (CPE), usually after 14–21 days, cells were harvested and subjected to three freeze–thaw cycles, followed by centrifugation to remove cellular debris, and the resulting supernatant (2 ml) used to infect a 100 mm dish of 90 % confluent AdHek cells. Following observation of CPEs after 2–3 days, viral particles were purified and expanded by infecting 10 plates of

AdHek cells. Finally, target MSCs, grown on 25 mm coverslips (5,000 cells/coverslip), were infected by addition of 1:500 of virus dilution, two days after, cells were ready for HyPer imaging.

Microscopy and imaging of HyPer biosensor

At the experimental day, medium was replaced by KRH buffer (in mM: 140 NaCl, 4.7 KCl, 20 Hepes, 1.25 $MgSO_4$, 1.25 $CaCl_2$, pH 7.4) supplemented with 5 mM glucose and the coverslip was mounted in an open recording chamber. Images of MSCs were registered using a Nikon Ti inverted microscope equipped with 40X oil objective [numerical aperture, N.A. 1.3]. A Xenon lamp was coupled to the monochromator device (Cairn Research Ltd, Faversham, UK). Digital images were acquired by means of a cooled CCD camera (Hamamatsu ORCA 03, Japan) and their analyses were performed using freeware micromanager software [Edelstein et al, 2014].

HyPer biosensor is assembled with permutated fluorescent proteins, corresponding to cyano fluorescent protein (CFP) excited at 420 nm and yellow fluorescent protein (YFP) excited at 490 nm. Ratiometric imaging requires dual excitation at 420 nm and 490 nm; whereas the emitted light should be collected with a long pass filter over 520 nm. Under this configuration, the biosensor signals from both excitation wavelengths were acquired each 20 seconds and converted in a ratio (490/420) making H_2O_2 measurements reliable and independent of the biosensor expression.

The protocol for oxidative challenge was applied on infected c- and o-MSCs as follow: At the beginning, HyPer ratio signal was recorded at least for 10 min to allow a stable behaviour. Then, a 50 μM H_2O_2 pulse was applied for the time indicated at the figure legends; after this, H_2O_2 was removed by changing for fresh KHR buffer leaving a time lapse, enough to allow recovery of the HyPer signal. Finally a pulse of 500 μM H_2O_2 was applied and recorded as before. Time-dependent changes in the fluorescence emitted by the HyPer biosensor were registered as explained above, and used to describe steady state parameters such as base line and peak responses to the 50 and 500 μM of H_2O_2 pulses.

Cell viability

For MSCs viability assays, 7.5×10^3 cells were seeded in 24 multiwell plates in culture medium containing different concentrations of H_20_2. After 2h of incubation, viability assays were performed using CellTiter 96® AQueous Non-Radioactive Cell Proliferation Assay (Promega, Madison, WI, USA) as recommended by the manufacturer. Absorbance was measured at 492 nm (Infinite 50, Tecan, Männedorf, Switzeland).

RNA Extraction and RT-qPCR

Cells were seeded at 8×10^4 cells per 35 mm diameter plate in basal medium for 72 hrs and then, followed by the treatment described by Chomcynski and Sacchi [1987] for RNA extraction. Briefly, treatment initiated with the removal of culture medium and addition of Trizol reagent (TRIzol, Life Technologies, California, USA), according to the manufacturer instructions. The RNA was quantified in a spectrophotometer (MBE2000, Perkin Elmer, Boston, MA, USA) and stored at -80°C. Reverse transcription was carried out with 1 μg

RNA, reverse transcriptase MMLV (Promega, Madison, WI, USA) and oligo dT (Promega, Madison, WI, USA) was performed according the following program; firstly RNA denaturation for 5 min at 72 °C, then 90 min cycle at 42 °C and a final cycle for 10 min at 72 °C.

Real-time PCR reactions were performed using 200 ng of cDNA in 10 μL of reaction mix according the instruction of FastStart Essential DNA Green Master kit (Roche Molecular Biochemicals, Mannheim, Germany). Reactions were performed in LightCycler®96 System (Roche Molecular Biochemicals, Mannheim, Germany). Relative gene expression was normalized to the housekeeping gene GAPDH and calculated using the formula 2 (Ct value of GAPDH - Ct value of gene of interest). The threshold cycle (Ct) was selected in the linear range of fluorescence for all genes. The primer sequence from forward to reverse 5' to 3' are: for catalase CTGACTACGGGAGCCACATC and AGATCCGGACTGCACAAAGG; for thioredoxin CTTGGACGCTGCAGGTGATA and TCCTGACAGTCATCCACATCT; for peroxiredoxin GGGAACCTGGTTGAACCCC and TGGCATAACAGCTGTGGCTT; for superoxide dismutase-1 CATTGCATCATTGGCCGCA and ACTTCCAGCGTTTCCTGTCTT; and for GADPH CAAAATCAAGTGGGGCGATGCTG and TGTGGTCATGAGTCCTTCCACGAT, respectively.

Statistical analysis.

The experiments were done in 4 different control and osteoporotic cell samples. Measurements of HyPer fluorescence were done in 33 and 39 single different c- and o-MSCs, respectively, derived from 4 different control and 4 different osteoporotic donors.

Data are expressed as the mean ± standard error and were analyzed by the Student's t-test or RM-ANOVA according to experimental design. p-value <0.05 was considered to be statistically significant.

Results

Expression of the biosensor HyPer by c- and o MSCs

After two days of treatment with the adenoviral vector, both c- and o-MSCs expressed the biosensor HyPer, There were fibroblastoid flat cells often larger than 100 μm in length, and these were observed by homogenous fluorescence at the cytoplasm (Fig 1A,C). Both types of MSCs were healthy, without traits of cellular stress or death. The functionality of the HyPer biosensor was tested by treating control and osteoporotic cells with 500 μM H_2O_2. A fast increase in the fluorescence emitted by cells followed the presence of the oxidant agent (figure 1B,D). No change in the characteristic appearance of cells was observed after the addition of hydrogen peroxide at the concentrations and time periods used in this report.

Upon the same oxidative challenge responses of c- and o MSCs expressing the biosensor HyPer are different.

To expose the antioxidant capacity of cells, c- and o-MSCs were challenged to two consecutives hydrogen peroxide pulses, leaving a temporal window in between to allow recovery of the HyPer signal, as indicated in methods. Representative temporal courses of

HyPer signal obtained from MSCs submitted to such oxidative sequence are shown in Figures 2A and 2B. At the beginning, HyPer signal showed to be stable enough to register a reliable base line. Then, subsequent to 50 μM H_2O_2 addition, the fluorescent signal ratio increased gradually and sustainably until reaching equilibrium. Next, H_2O_2 was removed from media by total buffer replacement and the HyPer signal diminished spontaneously attaining basal level (see figure 2A and 2B). In contrast, following the second 500 μM H_2O_2 pulse, a fast and noticeable rise in the HyPer signal was registered, reaching its maximal value almost instantaneously.

Data from the HyPer ratio obtained in all samples, are summarized as basal values (Figure 3A) and as percentage of the response at 50 μM H_2O_2 respect to maximal response at 500 μM H_2O_2 (Figure 3B). As shown, HyPer ratios at basal, and the maximum increase after 50 μM H_2O_2 pulse expressed in relation to the maximal value obtained at 500 μM, were similar in control and osteoporotic cells. On the other hand, the kinetic of HyPer response curves after adding 50 μM H_2O_2 to cells elicit different initial rates; for control cells the estimated rate was $0.037 \pm 0.003\ min^{-1}$, whereas for o-MSCs such parameter was estimates in $0.023 \pm 0.007\ min^{-1}$ (Fig 3C). Subsequently, the reach equilibrium was significant different between c- and o-MSCs. This parameter might integrate how fast exogenous H_2O_2 molecules effectively cross the plasma membrane and interact with the biosensor bypassing the diverse mechanisms committed in disulfide bond reduction, generically named here as antioxidant capacity. These values point to differences between both cells types in the integration of H_2O_2 way into cells and the several endogenous antioxidant mechanisms.

Considering the rapid decay in the HyPer signal following the last oxidative challenge, the kinetic of such recovery was compared in c- and o-MSCs. Results show that whereas c-MSCs exhibited a constant decay rate of $0.08 \pm 0.03\ min^{-1}$, the decay rate in o-MSCs was bimodal showing 2.8 fold faster than c-MSCs during the first minutes, with a decay rate of $0.22 \pm 0.01\ min^{-1}$. However, o-MSCs reached equilibrium at a remarkable higher ratio level than the recovery attained by c-MSCs (see dotted lines in Figure 3D).

The kinetic differences presented above suggest that some cellular components of o-MSCs are better prepared to avoid and restore undesired protein oxidation.

Levels of mRNAs for antioxidant agents in c- and o-MSCs.

The transcript levels for the enzymes catalase and SOD-1, and the proteins of the antioxidant defense system, thioredoxin and peroxiredoxin were measured by qRT-PCR in c- and o-MSCs. As shown in Figure 4, the transcript levels for enzymatic and non-enzymatic agents measured were higher in osteoporotic than in control cells. Thus, transcript levels for catalase, SOD-1, thioredoxin and peroxiredoxin were 9.9, 48.9, 18.8, and 3.6 fold higher in osteoporotic than in c-MSC, respectively (Figure 4). Accordingly, we then compared cells survival put up with an oxidant challenge in terms of its survival.

Short-term effect of hydrogen peroxide on MSCs cell viability.

Cell viability was measured after treating MSCs with increasing H_2O_2 concentrations, up to 1000 μM for 2h. The viability curves of c- and o-MSCs are shown in Figure 5; at H_2O_2 concentrations lower than 100 μM, viability of both cell types appeared increased; this effect

was more evident on c-MSCs (40%). At higher H_2O_2 concentrations, c-MSCs showed significantly sensitive to the oxidant, so that H_2O_2 at concentration higher than 250 μM decreased cell viability to values lower than 40%. In contrast, o-MSCs maintained 100% viability up to 1000 μM H_2O_2.

Discussion

Human multipotent MSCs have been reported to efficiently manage ROS *in vitro* through detoxifying enzymatic and non-enzymatic mechanisms [Valle-Prieto and Conget, 2010]. In this report, we analyzed in real time the response of individual MSCs to oxidative trials, by transducing the H_2O_2 specific fluorescent biosensor HyPer. Our results demonstrated that both, c- and o-MSCs, expressed the biosensor with a homogenous pattern of fluorescence through the cytoplasm, eliciting satisfactory signal to noise ratio in the recordings. Cells confronted with H_2O_2 challenges developed distinct responses in c- and o-MSCs, as noted from the biosensor HyPer's kinetics data. In fact, the oxidative insult was handled more efficiently by o-MSCs than c-MSCs cells. This conclusion was further supported by the increased levels of mRNAs for antioxidant proteins observed in o-MSCs, as well as by their improved resistance to H_2O_2 in terms of cell viability.

Since, we studied the cell response to an extracellular H_2O_2 bolus; the kinetics of HyPer signal increasing should give an account of both plasma membrane permeability to H_2O_2 and the cytosolic capacity to scavenge the incoming peroxide. Plasma membrane permeability to H_2O_2 greatly depends on the presence of water channels such as the aquaporins (AQPs); overexpression of AQP-3 in HEK293 cells allows recording of H_2O_2 at concentration as low as 10 μM [Miller et al, 2010], whereas silencing AQP-8 in HeLa cells totally inhibited H_2O_2 entry [Bertolotti et al, 2013]. In the case of human MSCs there is no report of AQPs mediating the peroxide flux through the plasma membrane. Our results indicated that MSCs facing the same 50 μM H_2O_2 oxidative treatment provoked a slower increase in the HyPer signal in o-MSCs than in c-MSCs, suggesting a further capacity to manage H_2O_2 in the former cells, compared to the known high antioxidant capacity of c-MSCs [Valle-Prieto and Conget, 2010]. Notwithstanding we cannot discard differences in cell membrane permeability to H_2O_2 in both types of MSCs.

Previously, the HyPer biosensor has been shown to be particularly useful to track the rate of signal recovery after successive H_2O_2 pulses, in primary hippocampal neurons [Porras and Stutzin, 2011]. Accordingly, in this study, the decay in the biosensor signal was recorded after removal of the H_2O_2 pulse. In o-MSCs, the rapid decrease in HyPer signal during the first minute could result from neutralization of residual intracellular H_2O_2 by the plentiful cytosolic peroxiredoxins, which can account for 80 % of micromolar peroxide in no more than 100 seconds [Moore et al, 1991; Chae et al, 1999]. Afterwards, disulfide bonds formed by the cysteine residues at the biosensor structure must be reduced by the glutaredoxin or thioredoxin systems, both with oxido-reductase activity in their cores [Chae et al, 1999]. In addition to the faster decay rate at very short-term in o-MSCs, it was notable that there was a high level of oxidized biosensor at which these cells reached equilibrium, compared to the reduced biosensor signal attained by c-MSCs, throughout an almost linear decay rate. Such difference cannot be explained by impaired thioredoxin in osteoporotic cells, based at least

on their higher expression of mRNA for thioredoxin-1 than c-MSCs. As an alternative, we postulate that o-MSCs adapted their functioning to a higher oxidation level. Therefore, in spite of their high antioxidant capacity, o-MSCs could have high tolerance to oxidized proteins by setting a high threshold for enzymatic reduction of undesirable disulfide bonds. Since ROS level appears to play a pivotal role in lineage commitment of MSCs, the former explanation agrees with the observation of impaired osteogenic differentiation in o-MSCs [Rodríguez et al, 2000; Hess et al, 2005], as osteogenesis is blunted by elevated ROS while inducing positively adipogenesis in MSCs and other adipogenic progenitors [Atashi et al, 2015; Kanda et al, 2011]. Since we and others have shown that MSCs from osteoporotic individuals are more likely to differentiate into adipocytes than osteoblasts, and osteoporotic women have increased bone marrow adiposity at the expense of the osteoblast, it is conceivable that the o-MSCs are entrained to handle more ROS because of their metabolic programming into the pre-adipogenic lineage.

Formerly, observations in rat and human MSCs have suggested that the basal antioxidant capacity of MSCs can be upregulated to prevent the accumulation of intracellular ROS [Valle-Prieto and Conget, 2010; Stolzing and Scutt, 2006; Ebert et al, 2006; Chen et al, 2008]; here we show that o-MSCs express significantly higher level of transcripts for SOD-1, catalase, thioredoxin, and peroxiredoxin than in c-MSCs, which may be an adaptive response of o-MSCs for maintaining stem cells self-renewing and differentiation potential under oxidative stringent conditions [Calzadilla et al, 2011; Chaudhari et al, 2014]. Therefore, up-regulated mechanisms for ROS neutralization in o-MSCs would be consistent with impaired activity for reducing protein disulfide bonds, thereby adjusting o-MSCs to a higher oxidative status than control cells. Such proposition is further substantiated by the dissimilar H_2O_2 toxic effect on both cell types; toxicity was significantly lower on o-MSCs than on c-MSCs, as reflected by maintained o-MSCs' cell viability after varying H_2O_2 treatment.

To our knowledge, this is the first report on the response in real time of individual h-MSCs to an oxidative challenge. Taken together, our results indicate that although o-MSCs have improved antioxidant capacity compared to control cells, the former adjust to withstand higher oxidative status. There are observations suggesting that in osteoporosis the conditions in the bone marrow microenvironment could sustained oxidative processes [Maggio et al, 2003; Feng and Tang, 2014; Pino et al, 2010], such metabolic context either transiently or chronically could take a part in modifying the cellular phenotype towards that of o-MSCs [Pino et al, 2012]. Mouzannar et al. [2011] demonstrated in embryonic stem cells *in vitro*, that a single short exposure to minimally toxic ROS produced significant alterations in cell metabolic programming, while cells maintained their stem cell traits.

In conclusion, our study adds support to the tenet that MSCs from osteoporotic individuals differs from healthy controls. Further studies are needed to precise the metabolic consequences of oxidative adjustments in o-MSCs and whether they can be reversed by anti-oxidative agents.

Acknowledgment

This work was supported by grants from the Fondo Nacional de Ciencia y Tecnología: FONDECYT # 1130045 (JPR), # 1160214 (JPR) and #1120201 (OP).

Funding:

Grants Fondo Nacional de Ciencia y Tecnología, FONDECYT # 1130045 (JPR), #1160214 (JPR), #1120201 (OP)

References

Afonso V, Champy R, Mitrovic D, Collin P, Lomri A. 2007. Reactive oxygen species and superoxide dismutases: role in joint diseases. Joint Bone Spine 74: 324–329. [PubMed: 17590367]

Almeida M, Ambrogini E, Han L, Manolagas SC, Jilka RL. 2009. Increased lipid oxidation causes oxidative stress, increased PPARγ expression and diminished pro-osteogenic Wnt signaling in the skeleton. J Biol Chem 284: 27438–27448. [PubMed: 19657144]

Ambrogini E, Almeida M, Martin-Millan M, Paik JH, Depinho RA, Han L, Goellner J, Weinstein RS, Jilka RL, O'Brien CA, Manolagas SC. 2010. FoxO-mediated defense against oxidative stress in osteoblasts is indispensable for skeletal homeostasis in mice. Cell Metab 11(2): 136–146. [PubMed: 20142101]

Astudillo P, Ríos S, Pastenes L, Pino AM, Rodríguez JP. 2008. Increased adipogenesis of osteoporotic human-mesenchymal stem cells (MSCs) characterizes by impaired leptin action. J Cell Biochem 103: 1054–1065. [PubMed: 17973271]

Atashi F, Modarressi A, Pepper MS. 2015. The Role of Reactive Oxygen Species in Mesenchymal Stem Cell Adipogenic and Osteogenic Differentiation: A Review. Stem Cells and Development 24(10): 1150–1163. [PubMed: 25603196]

Bai XC, Lu D, Liu AL, Zhang ZM, Li XM, Zou ZP, Zeng WS, Cheng BL, Luo SQ. 2005. Reactive oxygen species stimulates receptor activator of NF-kappaB ligand expression in osteoblast. J Biol Chem 29: 17497–17506.

Balaban RS, Nemoto S, Finkel T. 2005. Mitochondria, oxidants, and aging. Cell 120: 483–495. [PubMed: 15734681]

Basu S, Michaëlsson K, Olofsson H, Johansson S, Melhus H. 2001. Association between oxidative stress and bone mineral density. Biochem Biophys Res Commun 288: 275–279. [PubMed: 11594785]

Belousov VV, Fradkov AF, Lukyanov KA, Staroverov DB, Shakhbazov KS, Terskikh AV, Lukyanov S. 2006. Genetically encoded fluorescent indicator for intracellular hydrogen peroxide. Nature Methods 3 (4): 281–286. [PubMed: 16554833]

Bertolotti M, Bestetti S, García-Manteiga JM, Medraño-Fernandez I, Dal Mas A, Malosio ML, Sitia R. 2013. Tyrosine Kinase Signal Modulation: A Matter of H_2O_2 Membrane Permeability? Antioxid Redox Signal 19(13): 1447–1451. [PubMed: 23541115]

Calzadilla P, Sapochnik D, Cosentino S, Diz V, Dicelio L, Calvo JC, Guerra LN. 2011. N-Acetylcysteine Reduces Markers of Differentiation in 3T3-L1 Adipocytes. Int J Mol Sci 12: 6936–6951. [PubMed: 22072928]

Chae HZ, Kim HJ, Kang SW, Rhee SG. 1999. Characterization of three isoforms of mammalian peroxiredoxin that reduce peroxides in the presence of thioredoxin. Diabetes Research and Clinical Practice 45: 101–112. [PubMed: 10588361]

Chaudhari P, Ye Z, Jang Y-Y. 2014. Roles of reactive oxygen species in the fate of stem cells. Antioxid Redox Signal 20 (12): 1881–1890. [PubMed: 23066813]

Chen CT, Shih YR, Kuo TK, Lee OK, Wei YH. 2008. Coordinated changes of mitochondrial biogenesis and antioxidant enzymes during osteogenicdifferentiation of human mesenchymal stem cells. Stem Cells 26(4): 960–968. [PubMed: 18218821]

Chomczynski P, Sacchi N. 1987. Single-step method of RNA isolation by acid guanidinium thiocyanate-phenol-chloroform extraction. Anal Biochem 162: 156–159. [PubMed: 2440339]

Dalle-Donne I, Rossi R, Colombo R, Giustarini D, Milzani A. 2006. Biomarkers of oxidative damage in human disease. Clin Chem 52: 601–623. [PubMed: 16484333]

Ebert R, Ulmer M, Zeck S, Meissner-Weigl J, Schneider D, Stopper H, Schupp N, Kassem M, Jacob F. 2006. Selenium supplementation restores the antioxidative capacity and prevents cell damage in bone marrow stromal cells in vitro. Stem Cells 24: 1226–1235. [PubMed: 16424399]

Edelstein AD, Tsuchida MA, Amodaj N, Pinkard H, Vale RD, Stuurman N. 2014. Advanced methods of microscope control using μManager software. J Biol Methods 2014; 1(2): e10. DOI: 10.14440/jbm.2014.36.

Feng Y-L, Tang X-L. 2014. Effect of glucocorticoid-induced oxidative stress on the expression of Cbfa1 Chemico-Biological Interactions 207: 26–31. [PubMed: 24239970]

Filaire E, Toumib H. 2012. Reactive oxygen species and exercise on bone metabolism: Friend or enemy? Joint Bone Spine 79: 341–346. [PubMed: 22578961]

Giorgio M, Trinei M, Migliaccio E, Pelicci PG. 2007. Hydrogen peroxide: a metabolic by-product or a common mediator of ageing signals? Nat Rev Mol Cell Biol 8: 722–728. [PubMed: 17700625]

Harman D 1956. Aging: a theory based on free radical and radiation chemistry. J Gerontol 11: 298–300. [PubMed: 13332224]

Hess R, Pino AM, Ríos S, Fernández M, Rodríguez JP. 2005. High affinity leptin receptors are present in human mesenchymal stem cells (MSCs) derived from control and osteoporotic donors. J Cell Biochem 94(1): 50–57. [PubMed: 15517602]

Hofer EL, Labovsky V, La Russa V, Vallone VF, Honegger AE, Belloc CG, Wen HC, Bordenave RH, Bullorsky EO, Feldan L, Chasseing NA. 2010. Mesenchymal stromal cells, colony-forming unit fibroblasts, from bone marrow of untreated advanced breast and lung cancer patients suppress fibroblast colony formation from healthy marrow. Stem Cells Dev 19: 359–370. [PubMed: 19388812]

Iyer S, Ambrogini E, Bartell SM, Han L, Roberson PK, de Cabo R, Jilka RL, Weinstein RS, O'Brien CA, Manolagas SC, Almeida M. 2013. FOXOs attenuate bone formation by suppressing Wnt signaling. J Clin Invest 123(8): 3409–3419. [PubMed: 23867625]

Jaiswal N, Haynesworth SE, Caplan AI, Bruder SP. 1997. Osteogenic differentiation of purified culture-explanded human mesenchymal stem cells *in vitro*. J Cell Biochem 64: 295–312. [PubMed: 9027589]

Kalyanaraman B, Darley-Usmar V, Davies KJA, Dennery PA, Forman HJ, Grisham MB, Mann GE, Moore K, Roberts LJ, Ischiropoulos H. 2012. Measuring reactive oxygen and nitrogen species with fluorescent probes: Challenges and limitations, Free Radical Biology & Medicine 52: 1–6. [PubMed: 22027063]

Kanda Y, Hinata T, Kang SW, Watanabe Y. 2011. Reactive oxygen species mediate adipocyte differentiation in mesenchymal stem cells. Life Sci 89: 250–258. [PubMed: 21722651]

Kuhn NZ, Tuan RS. 2010. Regulation of stemness and stem cell niche of mesenchymal stem cells: implications in tumorigenesis and metastasis. J Cell Physiol 222: 268–277. [PubMed: 19847802]

Kultere B, Friedl G, Jandrositz A, Sánchez-Cabo F, Prokesch A, Paar C, Scheideler M, Windhager R, Preisegger KH, Trajanoski Z. 2007. Gene expression profiling of human mesenchymal stem cells derived from bone marrow during expansion and osteoblast differentiation. BMC Genomics 8: 70–84. [PubMed: 17352823]

Linares GR, Xing W, Govoni KE, Chen ST, Mohan S. 2009. Glutaredoxin 5 regulates osteoblast apoptosis by protecting against oxidative stress. Bone 44: 795–804. [PubMed: 19442627]

Lu T, Finkel T. 2008. Free radicals and senescence. Exp Cell Res 314: 1918–1922. [PubMed: 18282568]

Maggio D, Barabani M, Pierandrei M, Polidori MC, Catani M, Mecocci P, Senin U, Pacifici R, Cherubini A. 2003. Marked decrease in plasma antioxidants in aged osteoporotic women: results of a cross-sectional study. J Clin Endocrinol Metab 88: 1523–1527. [PubMed: 12679433]

Manolagas SC. 2010. From estrogen-centric to aging and oxidative stress: a revised perspective of the pathogenesis of osteoporosis. Endocr Rev 31(3): 266–300. [PubMed: 20051526]

Manolagas SC, Almeida M. 2007. Gone with the Wnts: beta-catenin, T-cell factor, forkhead box O, and oxidative stress in age-dependent diseases of bone, lipid, and glucose metabolism. Mol Endocrinol 21(11): 2605–2614. [PubMed: 17622581]

McBride SH, Falls T, Knothe Tate ML. 2008. Modulation of stem cell shape and fate B: mechanical modulation of cell shape and gene expression. Tissue Eng Part A 14: 1573–1580. [PubMed: 18774911]

McCord JM. 2000. The evolution of free radicals and oxidative stress. Am J Med 108: 652–659. [PubMed: 10856414]

Miller EW, Dickinson BC, Chang CJ. 2010. Aquaporin-3 mediates hydrogen peroxide uptake to regulate downstream intracellular signaling. Proc Natl Acad Sci 107(36): 15681–15686.MITRY. [PubMed: 20724658]

Moore RB, Mankad MV, Shriver SK, Vipul N, Mankad VN, Plishker GA. 1991. Reconstitution of Ca2+-dependenKt + Transport in Erythrocyte Membrane Vesicles Requires a Cytoplasmic Protein. J Biol Chem 266(28): 18964–18968. [PubMed: 1918011]

Mouzannar R, Mccafferty J, Benedetto G, Richardson C. 2011. Transcriptional and phospho-proteomic screens reveal stem cell activation of insulin-resistance and transformation pathways following a single minimally toxic episode of ROS. Int J Genomics Proteomics 2(1): 34–49. [PubMed: 21743783]

Oh B, Kim SY, Kim DJ, Lee JY, Lee JK, Kimm K, Park BL, Shin HD, Kim TH, Park EK, Koh JM, Kim GS. 2007. Associations of catalase gene polymorphisms with bone mineral density and bone turnover markers in postmenopausal women. J Med Genet 44:e62. [PubMed: 17209132]

Pino AM, Ríos S, Astudillo P, Fernández M, Figueroa P, Seitz G, Rodríguez. 2010. Concentration of adipogenic and pro inflammatory cytokines in the bone marrow supernatant fluid of osteoporotic women. J Bone Min Res 25: 492–498.

Pino AM, Rosen CJ, Rodríguez JP. 2012. In osteoporosis, differentiation of mesenchymal stem cells (MSCs) improves bone marrow adipogenesis. Biol Res 45: 81–89. [PubMed: 22688988]

Porras OH, Stutzin A. 2011. Glutamate-induced metabolic changes influence the cytoplasmic redox state of hippocampal neurons. Biochem Biophys Res Commun 2011: 411: 82–87.

Rached MT, Kode A, Xu L, Yoshikawa Y, Paik JH, Depinho RA, Kousteni S. 2010. FoxO1 is a positive regulator of bone formation by favoring protein synthesis and resistance to oxidative stress in osteoblasts. Cell Metab 11(2): 147–160. [PubMed: 20142102]

Raiz LG. 1997. The osteoporosis revolution. Ann Intern Med 126: 458–462. [PubMed: 9072932]

Rodríguez JP, Montecinos L, Ríos S, Reyes P, Martínez J. 2000. Mesenchymal stem cells from osteoporotic patients produce a type I collagen-deficient extracellular matrix favoring the adipogenic differentiation. J Cell Biochem 79: 557–565. [PubMed: 10996846]

Russell SJ, Kahn CR. 2007. Endocrine regulation of ageing. Nat Rev Mol Cell Biol 8: 681–691. [PubMed: 17684529]

Seebach C, Henrich D, Tewksbury R, Wilhelm K, Marzi I. 2007. Number and proliferative capacity of human mesenchymal stem cells are modulated positively in multiple trauma patients and negatively in atrophic nonunions. Calcif Tissue Int 80: 294–300. [PubMed: 17431529]

Serafini M 2006. The role of antioxidants in disease prevention. Medicine 34: 533–535.

Stolzing A, Scutt A. 2006. Effect of reduced culture temperature on antioxidant defenses of mesenchymal stem cells. Free Radic Biol Med 41: 326–338. [PubMed: 16814114]

Valko M, Leibfritz D, Moncol J, Cronin MTD, Mazur M, Telser J. 2007. Free radicals and antioxidants in normal physiological functions and human disease. Int J Biochem Cell Biol 39: 44–84. [PubMed: 16978905]

Valle-Prieto A, Conget PA. 2010. Human Mesenchymal Stem Cells Efficiently Manage Oxidative Stress. Stem Cells and Development 19(12): 1885–1893. [PubMed: 20380515]

Wang W, Zhang Y, Lu W, Liu K. 2015. Mitochondrial reactive oxygen species regulate adipocyte differentiation of mesenchymal stem cells in hematopoietic stress induced by arabinosylcytosine. PLoS One. 2015 3 13;10(3):e0120629. doi: 10.1371/journal.pone.0120629. eCollection 2015. [PubMed: 25768922]

Zhou S, Greenberger JS, Epperly MW, Goff JP, Adler C, Leboff MS, Glowacki J. 2008. Age-related intrinsic changes in human bonemarrow-derived mesenchymal stem cells and their diff erentiation to osteoblasts. Aging Cell 7: 335–343. [PubMed: 18248663]

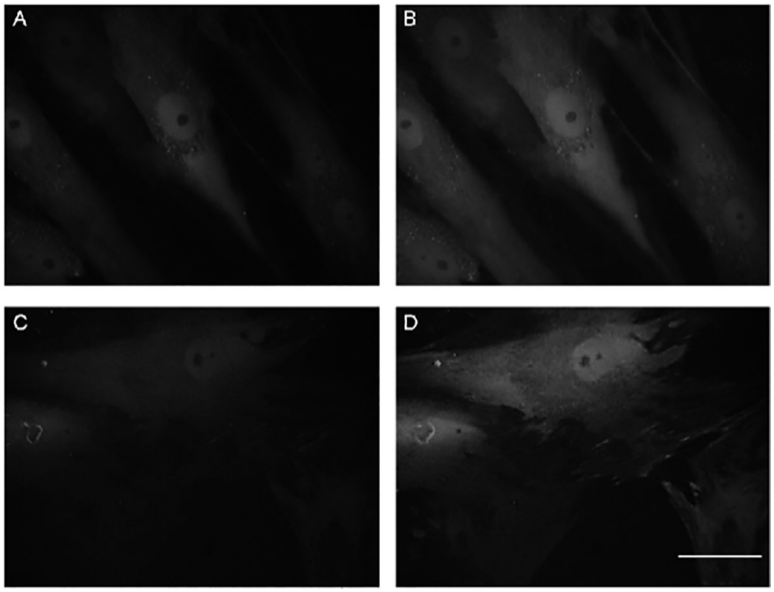

Figure 1.

Representative microphotographs of control- and osteoporotic-MSCs expressing the HyPer biosensor at cytoplasm. Images were obtained after two days of infection, as described in Materials and Methods, fluorescence from HyPer excitation at 490 nm. The same field of control-MSCs and osteoporotic-MSCs, respectively, are shown before (A,C) and after a 500μM H_2O_2 pulse (B,D). Bar: 50μm

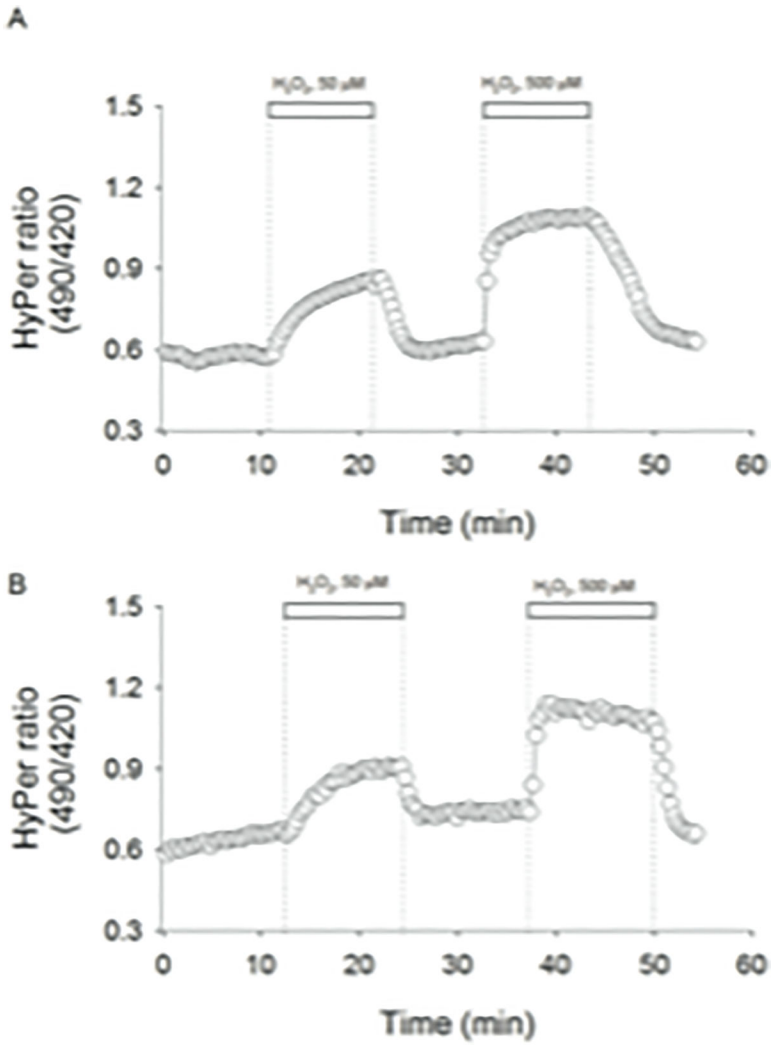

Figure 2.

Representative temporal courses of HyPer signal recorded from control **A)** and osteoporotic mesenchymal stem cells **B)**. Pulses of 50 μM and 500 μM H_2O_2 were applied, as indicated by white bars. Cells were excited at 420 nm and 490 nm, and emitted light was collected at 520 nm. Biosensor signals from both excitation wavelengths were acquired each 20 seconds and converted in a ratio (490/420).

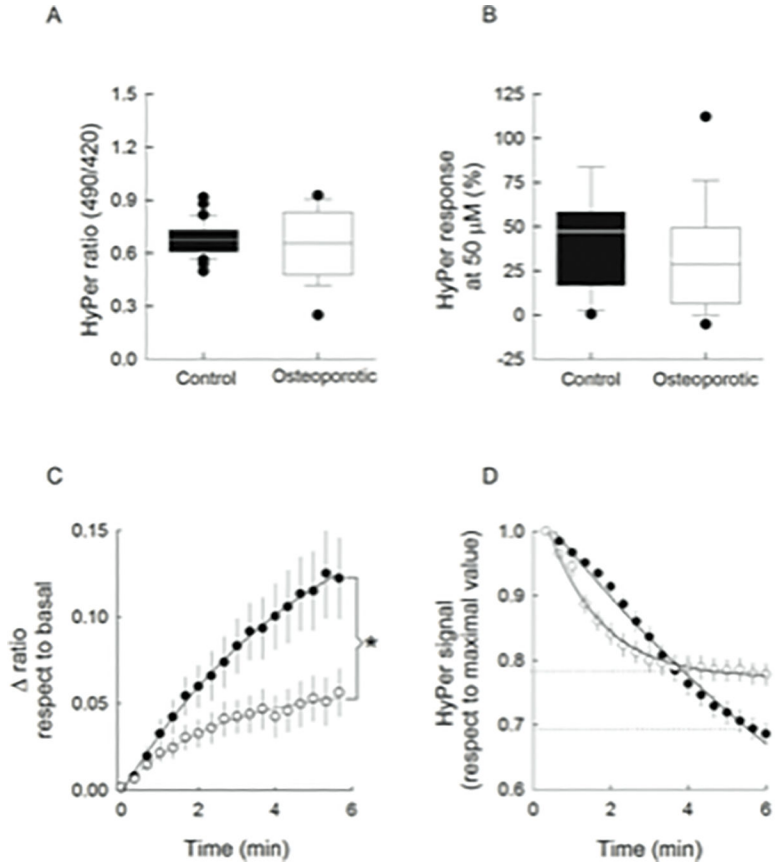

Figure 3.

Analysis of Data from MSCs expressing HyPer- exposed to H_2O_2 challenges. Data from base lines values **(A),** and of percentage of the HyPer response at 50 μM H_2O_2 pulse respect to the maximal value at 500 μM H_2O_2 pulse **(B),** for control (black boxes) and osteoporotic MSCs (white boxes). A line across the boxes indicates the median and error bars point out the 5^{th} and 95^{th} percentiles. Time course of the HyPer signal at 50 μM H_2O_2 respect to corresponding base line value, in c-MSCs (filled circles) and o-MSCs (open circles) **(C)**. *$p<0.05$, according to Mann-Whitney rank sum test HyPer signal decay after 500 μM H_2O_2 pulse from control (filled circles) and from osteoporotic MSCs (open circles) **(D)**. Dotted lines indicate the equilibrium attained by both cell types. Data were fitted to exponential functions and correspond to the mean ± SE. All data were obtained from 33 individual control cells from 4 different donors and from 39 individual osteoporotic cells from 4 different donors.

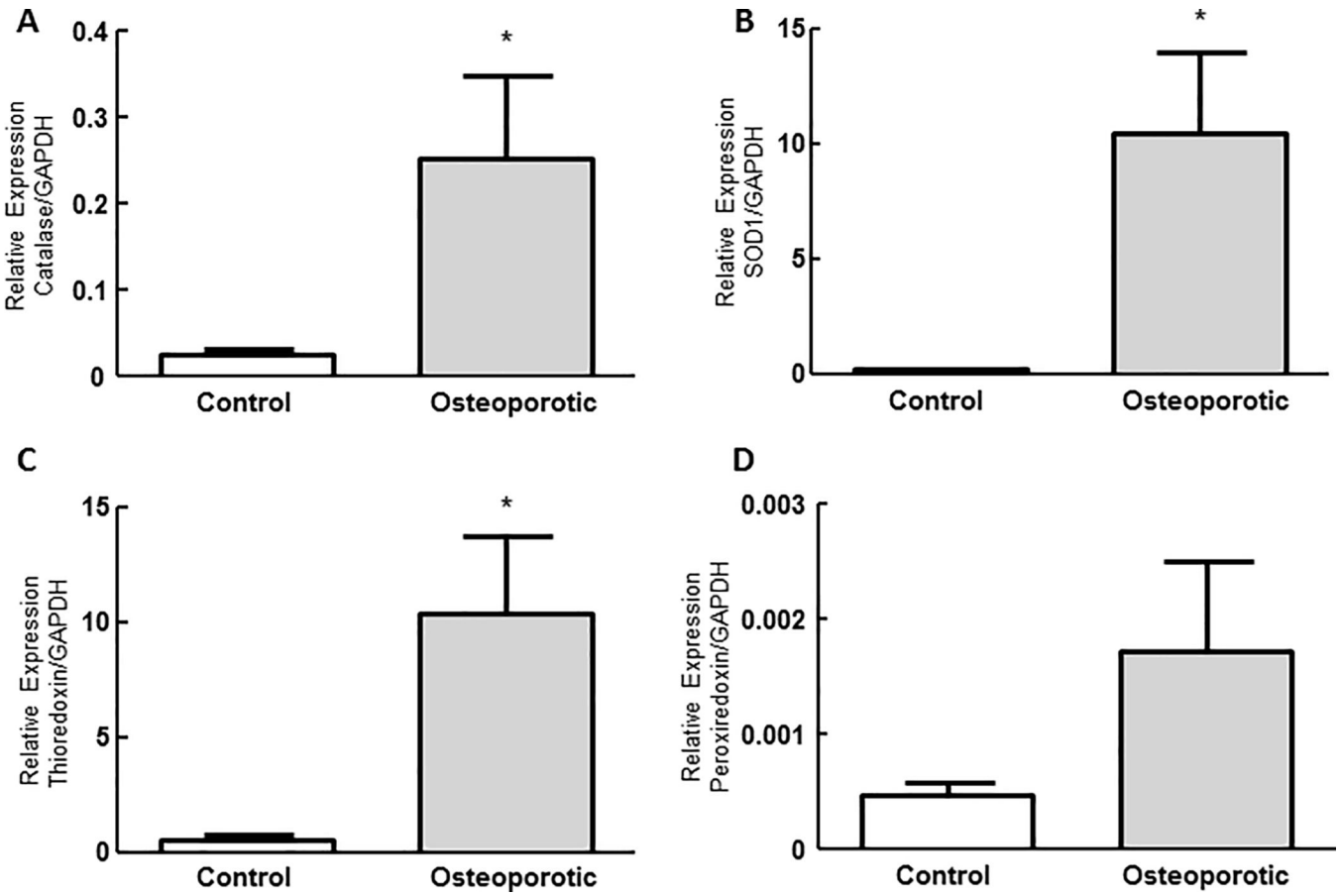

Figure 4.

Measurement of transcript levels for antioxidant agents. Transcript levels of catalase **(A)**, superoxide dismutase 1 **(B)**, thioredoxin **(C)**, peroxiredoxin **(D)** were measured by qRT-PCR as described in Materials and Methods. GADPH was used as housekeeping gene. Results are expressed as mean ± SE from 4 different control and osteoporotic samples. Measurements were performed in duplicate. *$p<0.05$, unpaired t-student.

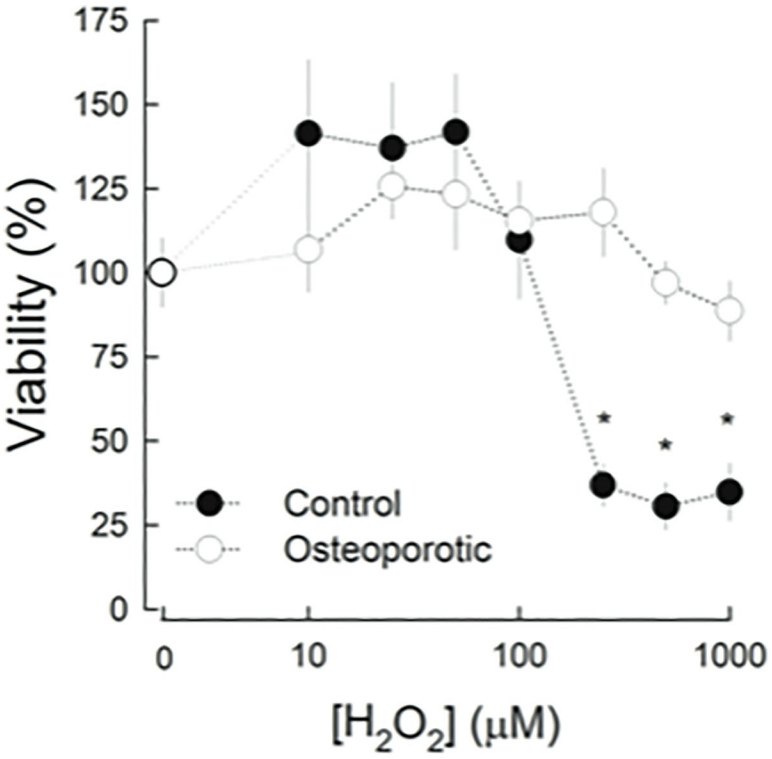

Figure 5.

Viability of MSCs after H_2O_2 treatment. MSCs were incubated during 2 h with indicated H_2O_2 concentrations. Viable cells were determined as indicated in Materials and Methods and expressed as percentage of cells in the absence of peroxide. Filled circles correspond to control-MSCs and, open circles to osteoporotic-MSCs. Results are expressed as mean ± SE from 4 different control and ostoporotic samples. Experiments were performed in triplicate. * $p<0.05$, Kruskal-Wallis One Way Analysis of Variance.

Table 1.

Demographic and Densitometric Characteristics of Donors (n=8)

Demographic Data	Control (n=4)	Osteoporotic (n=4)
Age (years)	72.2 ± 6.5	72.4 ± 7.3
Height (cm)	153.4 ± 5.9	152.9 ± 6.2
Weight (kg)	61.8 ± 9.3	68.7 ± 11.5
BMI	26.2 ± 3.2	29.0 ± 5.1
t-score (L2-L4)	−0.58 ± 1.3	−3.33 ± 0.8 *
BMD (g/cm^2)	1.118 ± 0.13	0.811 ± 0.11 *

BMI, body mass index; BMD, bone mass density. Results are expressed as mean ± standard deviation.

* $p<0.01$, between control and osteoporotic donors.